Chapter

Density Functional Theory Study of the Solvent Effects on Electronic Transition Energies of Porphyrins

Metin Aydin

Abstract

We have calculated the solvent effects on the ground state and the lowest triplet state absorption spectra of *meso*-tetraphenylporphyrin (TPP), meso-tetrakis(*p*-sulfonatophenyl)porphyrin (TSPP) and their diprotonated forms (H_4TPP and H_4TSPP) in thirty-nine different solvent using time-dependent-DFT density functional theory (TD-DFT) coupled with CPCM method. The results of the calculations show that the Q-bands and Soret-bands (or B-bands) in the absorption spectra of these compounds substantially change as function of solvent dielectric constant (ε) up to 20.493 (acetone), but become stabile in high polar solvents with dielectric constants $\varepsilon > 20$. The relative shifts in the B-bands are more significant than that in the Q-bands. The magnitude of the shifts in the spectral position of the Q and B bands are in the following order: H_4TSPP > H_4TPP > TPP > TSPP for the B-bands and H_4TSPP > H_4TPP > TSPP > TPP for the Q-bands. We also have determined that the energy-gaps between the B/Q-bands and their nearest triplet states are also solvent dependent for $\varepsilon < \sim 20.493$.

Keywords: porphyrin, TPP/TSPP, absorption, solvent effect, DFT

1. Introduction

Porphyrins are tetrapyrrolic macrocycles with conjugated electronic systems that exist in nature and have a large number of applications in several fields of research from biomedicine to materials science. The ubiquity of porphyrins in natural systems and their subtle yet important biological and chemical functions have inspired scientists to explore the unique structure/dynamics characteristics of compounds of this family, and to endeavor to imitate their properties in synthetic molecular analogs that display efficient use of solar energy [1–5] and could be used as active elements in molecular electronic devices [6, 7]. Furthermore, in recent times, porphyrin-like molecular systems have drawn a great deal of interest due to the use of therapeutic drugs, photosensitizers in photodynamic therapy of cancer [8], several applications in the treatment of nonmalignant conditions such as psoriasis, blocked arteries and pathological and bacterial infections [9], as well as in HIV research [10]. As known, biological effects of porphyrins generally derive from their photophysical and physicochemical properties, such as the

formation of molecular aggregates and axial ligation that give rise to significant modifications in absorption spectra, quantum yields, and fluorescence and triplet state lifetimes [11–15].

Along with rapid development in computer technology and computational quantum chemical methods, molecular properties have been intensively investigated in gas-phase and solvent-phase. Computational quantum chemistry is a powerful tool for understanding real-world chemical problems. Several molecular properties can be obtained by solving quantum mechanical equations. When the results of calculations are in agreement with their experimental results, we can interpret the experimental results more reasonably. Computational studies are not only performed to provide an understanding of experimental data, for instance the position and source of spectroscopic peaks, but also may be used to explore reaction mechanisms and molecular environment effect on the molecular properties.

Photophysical and photochemical properties of porphyrin and its derivatives have been widely studied by experimentalists and theoreticians [16–19]. Dipole allowed electronic excitation spectra of porphyrin compounds exhibit two major absorption bands in which are called as the Q-band in the visible region and the Soret band (or B-band) in the near UV region [20]; both of which have been the subject for a number of quantum chemical studies [21–29]. It has been experimentally reported that when porphyrin molecules are excited in the Soret- or B-band region, internal conversion (IC) takes place from the B-band to the Q-band, which is then followed by a fluorescence from the Q-band to the ground state S_0; i.e., $S_0 + h\nu_0 \rightarrow S_2(\text{B-band}) \rightarrow S_1(\text{Q-band}) \rightarrow S_0 + h\nu$. During relaxation of the S_1 state, a fraction of molecules also relaxes to the triplet T_1 via intersystem crossing (ISC).

The electrostatic interaction between a molecular system and its surrounding environment leads to change in geometric and spectroscopic properties. For instance, Jun Takeda and Mitsuo Sato [30] have experimentally studied solvent effect on the absorption spectra of meso-tetraphenylporphyrin (TPP) and dodecaphenylporphyrin (H_2DPP) in thirty-seven different neat solvent. The authors reported that the solvent leads to red shifts in Q-bands and B-band (Soret-band) in their absorption spectra, and that red shifts in H_2DPP are greater than those in TPP due to the nonplanarity of the H_2DPP macrocycle. The authors concluded that these red shifts in the absorption spectra of both compounds are caused by the hydrogen-bonding interactions of pyrrole NH protons and pyrrolenine nitrogen lone pairs with solvent.

Li Ye [31] used steady-state and time-resolved spectroscopic techniques to investigate photophysical properties of several metalloporphyrins have been examined in several different solvents. The author reported that the absorption spectrum of the Cu(TPPCl_8) in nonpolar solvents does not display a shift in the spectral position of the absorption bands and there is no evidence found for charge transfer (CT) transitions in the visible or near UV regions, however, in the polar solvent, blue shifts are observed in the absorption spectrum of the Cu(TPPCl_8) an intramolecular CT band takes place in absorption spectra. The author concluded that the activation free energy of the charge-transfer transition decreases with increasing outer reorganizational energy owing to increasing solvent polarity.

In order to take the solvent effect on the molecular properties into account in calculations, a number of implicit (continuum) theoretical models have been developed in the last decade, such as the polarizable continuum model (PCM), the dielectric PCM (DPCM), conductor-like PCM (CPCM), integral equation formalism PCM (IEFPCM), and the conductor-like screening model (COSMO)); see refs. [32, 33] for more details. Density functional theory (DFT) and Time-dependent DFT (TD-DFT) coupled with one of the PCM methods, which is becoming a

general routine in most quantum chemical software packages like Gaussian, can be used to compute solvent effect on the geometric and spectroscopic properties [34–37]. Results from such calculations has been shown to be successful in supporting analyses of experimental data with useful insights for better understanding of photophysical and photochemical pathways in solution.

L. Edwards et al. [38] have experimentally studied solvent effect on the spectral positions of dipole allowed singlet-singlet transitions ($S_0 \rightarrow S_n$) of the free-base porphyrin (FBP). Their experimental results shows that the Q-bands at 626 and 512 nm and the Soret band at 372 nm in gas-phase spectrum were respectively significantly shifted to 614, 519 and 391 nm in ethanol.

As far as we know, there is no theoretical study systematically investigating the solvent effect on porphyrin compounds in the literature, except our previous work [39] where we have studied solvent effect on the absorption spectra of the free-base porphyrin (FBP) and diprotonated form (H_4FBP) in the ground state and the lowest triplet state by using TD-DFT/CPCM techniques in thirty-nine different solvent (with solvent dielectric constant (ε) changes from 1 to 181.56). The results from calculations show that dipole allowed electronic transitions in each absorption spectrum change as function of increasing solvent dielectric constant up to about ε = 20.493 and remain almost constant with further increment of the solvent dielectric constant. We have also studied meso- substitution effect on the absorption spectra of the porphyrin (parent porphyrin) such as the meso-tetraphenylporphyrin (TPP), mesotetrakis (p-sulfonatophenyl) porphyrin (TSPP) and their diprotonated forms (H_4TPP and H_4TSPP), where the results from the calculations have shown that the meso-substituted functional groups result in a significant read shift in the electronic transition energies in the porphyrin absorption spectrum [19, 40].

This *work is a continuation* of our previous studies as mentioned above. In this present work we used TD-DFT/CPCM method to investigated solvent effect on the singlet-singlet and triplet-triplet electronic spectra of the TPP, TSPP and their protonated derivatives (H_4TPP and H_4TSPP).

2. Calculation section

The singlet-singlet and triplet-triplet electronic absorption spectra of the porphyrins and their derivatives in the gas phase and thirty-eight solvents were calculated using the Gaussian 09 software package [41]. Geometries for the ground and the lowest triplet states in each solvent were optimized using unrestricted density functional theory (at B3LYP level) [42, 43] with the 6-311G(d,p) basis set for C and H atoms and 6-311 + G(d.p) basis set [44] used for N, O and S atoms. Solvent effects were taken into account using self-consistent reaction field (SCRF) calculations [45], with the conductor-like polarizable continuum model (CPCM) [46–48] as contained in the Gaussian 09 software package. Type of solvent used in calculations are listed in **Table 1**. All compounds in both gaseous and solvents phases were optimized to minima on their ground and lowest triplet state potential energy surfaces (PESs) that is verified by the absence of imaginary frequencies in calculated vibrational spectra.

Time-dependent-DFT (at TD-B3LYP level) coupled with CPCM solvation method was used to calculate the first 24 singlet-singlet vertical electronic transitions ($S_0 \rightarrow S_n$) and 25 triplet-triplet vertical electronic transitions ($T_1 \rightarrow T_m$) in the gas and solvent phases. The GaussSum 0.8 freeware program [49] was used to check outputs and to generate computed absorption spectra from the output file of the Gaussian 09 software.

Solvent	ε	Solvent	ε	Solvent	ε
Gas	1.000	Bromoform	4.249	Acetone	20.493
Argon	1.430	Chloroform	4.711	1-Nitropropane	23.730
Krypton	1.519	Diiodomethane	5.320	Ethanol	24.852
Xenon	1.706	Chlorobenzene	5.697	Nitroethane	28.290
Heptane	1.911	Aniline	6.888	Methanol	32.613
Cyclohexane	2.017	Tetrahydrofuran	7.426	Nitrobenzene	34.809
Carbontetrachloride	2.228	Ethylmethanoate	8.331	Nitromethane	36.562
Benzene	2.271	Dichloromethane	8.930	1,2-Ethanediol	40.245
Toluene	2.374	Dichloroethane	10.125	Dimethylsulfoxide	46.826
Carbondisulfide	2.611	Benzylalcohol	12.457	Formicacid	51.100
Dibutylether	3.047	Cyclohexanone	15.619	Water	78.355
Propanoicacid	3.440	Cyclopentanol	16.989	Formamide	108.940
Diphenylether	3.730	Propanal	18.500	n-Methylformamide-mixture	181.560

Table 1.
The list of the solvents with their dielectric constants (ε) used in this work.

Additionally, we obtained a best fit to the calculated relative shifts in the Q and B bands positions by using the following equation: $f(\varepsilon) = \sum_n^5 C_n \left[\frac{(\varepsilon-1)}{(\varepsilon)}\right]^n$, where ε is the dielectric constant of the solvent and C_n is a constant. We would like to point out that $\frac{(\varepsilon-1)}{\varepsilon}$ in the fitting equations is part of the solvent correction in the CPCM method.

3. Results and calculations

3.1 Solvent dependence of TPP

It has been reported in literature that the measured absorption spectra of the TPP considerably depend on the dielectric constant of the solvent. For instance, the experimentally measured absorption spectrum the TPP exhibited the Soret-band at 398 nm in a pulsed supersonic expansion of helium [50], which is considerably shifted to 420 nm in toluene (ε = 2.374) [51], 419 nm in benzene (ε = 2.271) [52], 417 nm in *tetrahydrofuran* (ε = 7.426) and 415 nm in acetone (ε = 20.493) [51]. The Q(0-0) bands have been measured at 529 and 640 nm in a pulsed supersonic expansion of helium [50], which are also significantly shifted to 548 and 647 nm in benzene [52]. Furthermore, the lowest triplet state (T_1) of TPP at 77 K in methyl-cyclohexane [53] and diethyl ether/petroleum ether/isopropyl alcohol (in the ratio of 5/5/2) [54] was observed at 865 nm and 859 nm, respectively. The triplet-triplet absorption transitions of TPP in toluene were experimentally observed at 780, 690, 430, 405 and 390 nm [55].

It is worthy to note that the geometric structures of the TPP molecule both in the ground state and the lowest triplet state belong to the C_{2v} symmetry point group. The calculated solvent effect on the electronic spectrum of the TPP are summarized below.

Singlet TPP: Figure 1A provides the calculated absorption spectra of FBP in the different solutions used. The shifts in spectral positions of the Q, B (Soret) and L bands caused by the solvent are given in **Figure 1B** as functions of the dielectric constant of the solvent (ε).

The calculations indicate that the solvent effect on the Q1 and Q2 bands of the TPP are inconsequential. For instance, the Q1 band at 17398 cm^{-1} (574.8 nm) and Q2-band at 18566 cm^{-1} (538.6 nm) in gas-phase spectrum are 40 and 90 cm^{-1} red shifted to 17358 (576 nm) and 18473 cm^{-1} (541.4 nm), respectively, with increase in ε from 1.00 to 5.32; which then increased and become almost constant at around 17384 and 18506 cm^{-1} for ε > 20.493. However, the dependence of the calculated Soret bands (B1 and B2-bands) of the TPP significantly depend on solvent polarity. For example the B1 band at 25405 cm^{-1} (393.6 nm) and B2 band 26271 cm^{-1} (380.6 nm) in the gas phase spectrum initially decreased to 23890 (418.6 nm) and 24160 cm^{-1} (414.4 nm), respectively, with increase of ε from 1 to 5.32, and then blue-shifted to 23890 cm^{-1} (418.6 nm) and 24131 cm^{-1} (414.4 nm), respectively, for ε = 20.493 (acetone). With further increase in the dielectric constant (ε > 20.493), these bands positions become nearly stable at around 24574 (406.9, B1) and 24919 cm^{-1} (401.3 nm, B2) within 120 cm^{-1} fluctuations.

Similar to the modification in the positions of the B-bands, the spectral position of the L-band at 28862 cm^{-1} (346.5 nm) in the gas-phase (ε = 1.00) is first red-shifted to 28212 cm^{-1} (354.5 nm) in region of ε = 1 to 5.324, then blue-shifted to 29067 cm^{-1} (334 nm) for ε = 20.493, and then remains unchanged at 28334 cm^{-1} (352.9 nm) within ±20 cm^{-1} variation with the further increase in ε (**Figure 1**).

Triplet TPP: The lowest triplet state T_1 of the TPP in both gas-phase and solvent phase was estimated from calculated global energy difference between the singlet ground state and the lowest triplet state, i.e., E(T_1) = E(the global energy of the lowest triplet state)- E(the global energy of the ground state). The energy level of the T_1 state of the TPP in the gas phase lies about 11406 cm^{-1} (876.8 nm) above the ground state energy (S_0). The estimated solvent effect on the energy gap between S_0-T_1 states is inconsequential, only about 20 cm^{-1} red-shifted with increasing solvent polarity (see **Figure 2B**).

The calculated triplet-triplet electronic transitions up to 25000 cm^{-1} (400 nm) are given in **Figure 2(A** and **B)**. The calculations indicate that the triplet states

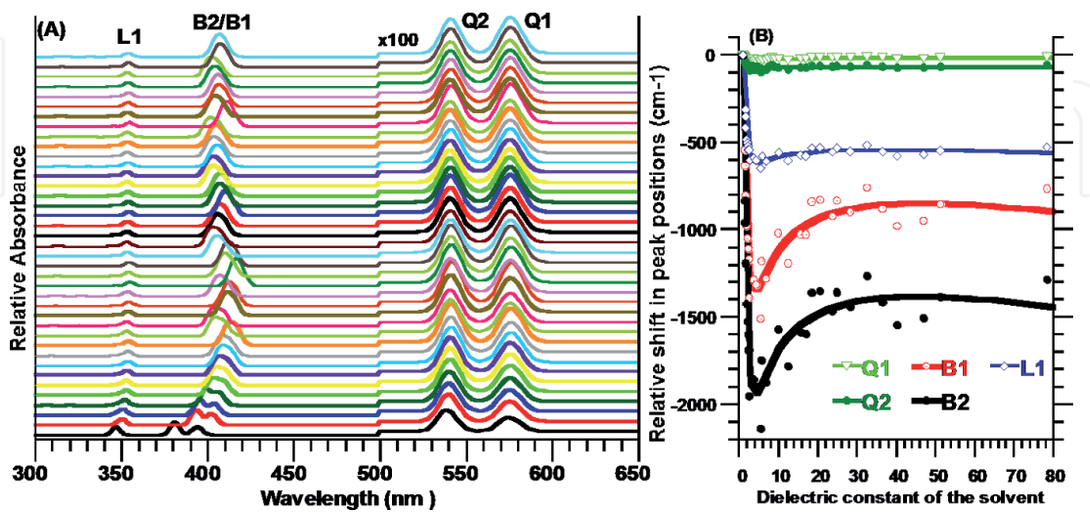

Figure 1.
(A) The calculated solvent-dependence of the singlet-singlet electronic absorption spectrum of the TPP in the thirty-nine different environments, where the dielectric constant of the molecular environment increases from bottom (ε = 1.00) to top (ε = 181.560); (B): The shift in the positions of the Q1, Q2, B1, B2 and L1 bands reference to their corresponding values in gas-phase spectrum as function of dielectric constant of the solvent (ε).

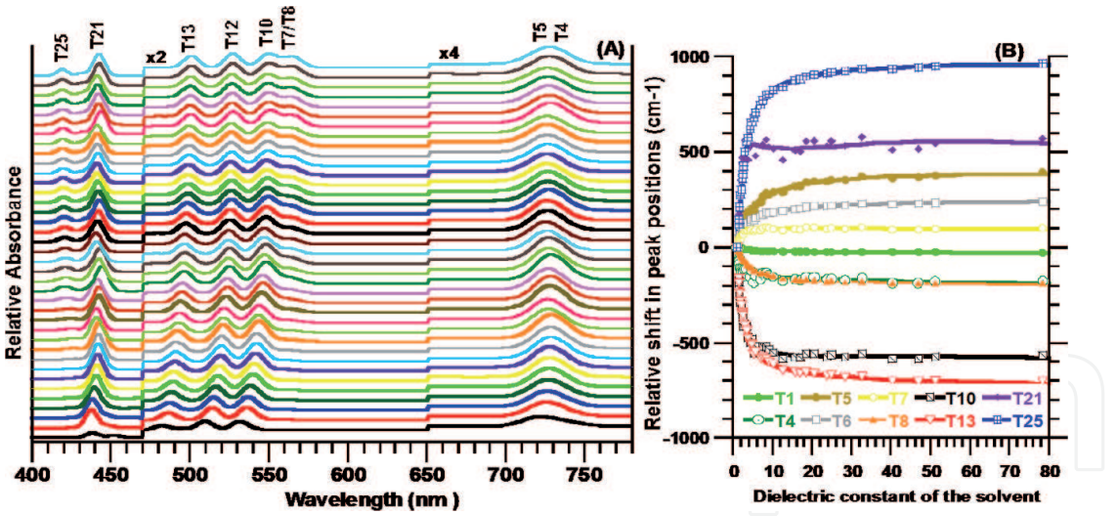

Figure 2.
(A) The calculated solvent-dependence of the triplet-triplet electronic absorption spectrum of the TPP in the thirty-nine different environments, where the dielectric constant of the molecular environment increases from bottom (ε = 1.00) to top (ε = 181.560); (B): The shift in the energy level of the T_n state reference to their corresponding value in gas-phase spectrum as function of dielectric constant of the solvent (ε). The shift in the energy level of the T_1 state: $\Delta E(T_1,\varepsilon) = E(T_1,\varepsilon)-E(S_0,\varepsilon)$.

at 18805 cm^{-1} (531.8 nm; labeled as T_{10}) and 20722 cm^{-1} (482.6 nm, T_{13}) in the gas-phase spectrum of the TPP are gradually red-shifted to 18232 and 20041 cm^{-1} (or 548.5 and 499.0 nm) as a function of ε up to 28.29), respectively, and become stable within a few wavenumbers variation with the further increment in solvent dielectric constant (ε). On contrary to red-shifts in the energy level of the T_{10} and T_{13} states, the T_{21} (at 22130 cm^{-1}/451.9 nm) and T_{25} (22926 cm^{-1}/436.2 nm) in the gas-phase are blue-shift to 22666 cm^{-1} (441.2 nm) and 23849 cm^{-1} (419.3 nm), respectively, as function of ε up to 28.29. Additionally, the solvent leads to blue shifts (around 400 cm^{-1}) and red shifts (about 200 cm^{-1}) in the calculated energy levels of other triplet states as seen in see **Figure 2B**.

The İntersystem crossing (ISC) between singlet and triplet excited states of a molecular system is very important for many purposes in photochemistry. Therefore, we also investigated solvent effect on the energy barrier between singlet and triplet state, ΔE(ISC) = E(triplet)-E(singlet), where the ISC may take place.

The results from calculations show that the energy gap between Q2-band and T_3 triplet state regularly decreases to −4 cm^{-1} (ε = 10.125) from −330 cm^{-1} (in gas-phase) with increasing solvent polarity and then slowly increases up to 60 cm^{-1} with the increase solvent polarity up to ε = 78.355. The gap between B2 band and T_4 triplet state rapidly decreases from −972 cm^{-1} in the gas phase to −84 cm^{-1} in Xenon (ε = 1.706), increases from 132 cm^{-1} (ε = 1.911) to a maximum value of 972 cm^{-1} (ε = 5.32), then follow an exponentially decrease to 110 cm^{-1} (ε = 78.355). The triplet state T_7 lies about 191 cm^{-1} above the L1-band in gas-phase, which start to decrease to 130 cm^{-1} with increase in the ε.

3.2 Solvent dependence of the H_4TPP

The UV–vis absorption spectrum of the diprotonated TPP (H_4TPP) exhibited a Soret band (B-band) at 22272 cm^{-1} (449 nm) in *acidic* chloroform solutions [56], 22831 cm^{-1} (438 nm) in acidic dichloromethane solution [57], 23419 cm^{-1} (427 nm) in acidified THF solution [58], and 22422 cm^{-1} (446 nm) *and* 22272 cm^{-1} (*449* nm) in acidic dichloromethane solution containing chloride *anion* (Cl^-) and bromide anion (Br^-), respectively [59]. The Q(0,0)-band was observed at 14837 cm^{-1} (674 nm) in acidic chloroform solutions [56], 15337 cm^{-1} (652 nm) in acidic

dichloromethane solution [57], 15432 cm^{-1} (648 nm) in acidic (H_2SO_4) dichloromethane solution, and 15129 cm^{-1} (661 nm) *in* acidic (H_2SO_4) dichloromethane solution containing chloride *anion* (Cl^-) [59]. These experimental results reveal that the solvent's polarity has significantly effects on the absorption spectrum of diprotonated TPP (H_4TPP). The calculated solvent effect on the absorption spectra of the H4TPP in thirty nine different solutions can summarized as follows.

Singlet H_4TPP: On contrary to red-shifts of the bands in the absorption spectrum TPP, the solvent leads to substantial blue-shifts of the absorption bands in the protonated TPP (H_4TPP) spectrum as seen in **Figure 3(A** and **B)**. For instance, the calculated Q (14761 cm^{-1}/ 677.5 nm), B (20583 cm^{-1}/485.8 nm), L1 (21803 cm^{-1}/458.7 nm), L2 (24095 cm^{-1}/415.0 nm) and M (28465 cm^{-1}/351.3 nm) bands in gas phase spectrum are progressively blue shifted to 15352, 22981, 25069, 25731, and 29355 cm^{-1} (or 651.4, 435.2, 404.4, 398.9 and 388.6 nm), respectively, as function of solvent dielectric constant (ε) from 1.00 to 20.493. With further increase in ε, these electronic bands remain almost constant within a few ten of wavenumbers fluctuation. These calculated results are consistent with the experimentally observed dependence of the absorption spectrum of H4TPP on molecular environments as discussed above.

Triplet H_4TPP: While **Figure 4(A)** provides the calculated electronic spectra of the triplet H_4TPP in the solvents used in this work, **Figure 4B** provides the shifts in the peak positions as function of the solvent dielectric constant relative to their corresponding positions in the gas phase spectrum. The results from calculations show that the solvent gives rise to change in dipole allowed triplet-triplet vertical electronic transition energies in the H_4TPP spectrum as well energy level of the lowest triplet state (T_1) as a function of solvent dielectric constant only in the region of solvent dielectric constant from ε = 1 to 28.493 and, with further increase of solvent dielectric constant, remain unchanged within a few wavenumber variations, see **Figure 4A** and **B**. Therefore, we only provide the maximum shifts when molecular environment changes from the gas phase to acetone (ε = 28.493). It is worthy to point that the shift in the energy level of the lowest triplet state (T_1) was estimated from the equation: $\Delta E(T_1,\varepsilon) = E(T_1,\varepsilon)-E(S_0,\varepsilon)$.

The predicted T_1 lowest triplet state gradually blue shifts from 8232 cm^{-1} (1215 nm) in gas phase to 8767 cm^{-1} (1141 nm) in acetone solvent medium. The T_4

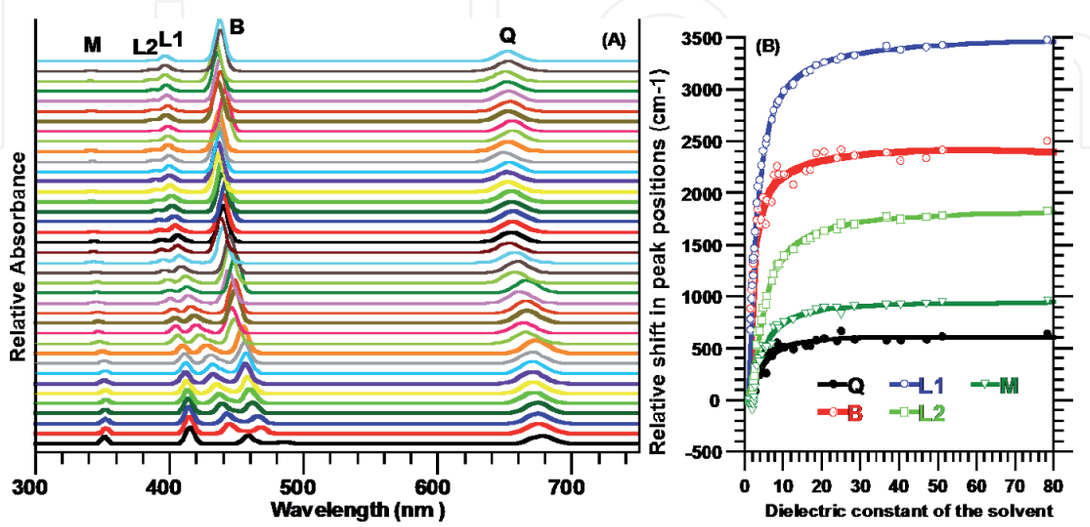

Figure 3.
(A) The calculated solvent-dependence of the singlet-singlet electronic absorption spectrum of the H_4TPP in the thirty-nine different environments, where the dielectric constant of the molecular environment increases from bottom (ε = 1.00) to top (ε = 181.560); (B): The red-shifts in the absorption band positions as function of dielectric constant of the solvent (ε), reference to their corresponding values in gas-phase spectrum.

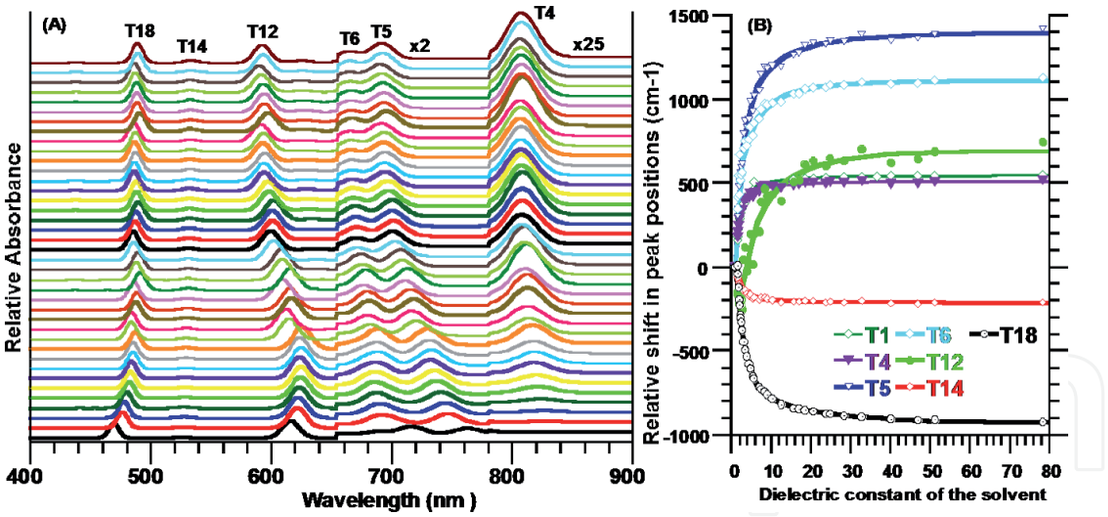

Figure 4.
(A) The calculated solvent-dependence of the triplet-triplet electronic absorption spectrum of the H_4TPP in the thirty-nine different environments, where the dielectric constant of the molecular environment increases from bottom (ε = 1.00) to top (ε = 181.560); (B): The shift in the energy level of the T_n state reference to their corresponding value in gas-phase spectrum as function of dielectric constant of the solvent (ε). The shift in the energy level of the T_1 state is obtained using the equation: $\Delta E(T_1,\varepsilon) = E(T_1,\varepsilon)-E(S_0,\varepsilon)$.

(at 11900 cm^{-1}/840.3 nm), T_5 (13093 cm^{-1}/763.8 nm), T_6 (13955 cm^{-1}/716.6 nm), T_7 (13291 cm^{-1}/752.4 nm), and T_{12} (16236 cm^{-1}/615.9 nm) in the gas phase spectrum are 500, 1344, 1083, 2176, and 631 cm^{-1} blue shifted in spectrum of H_4TPP in acetone, respectively. However, the T_{14} (19024 cm^{-1}/525.7 nm) and T_{18} (21607 cm^{-1}/462.8 nm) are 210 and 890 cm^{-1} red shifted in acetone as solvent, respectively, see **Figure 4A** and **B**.

The SCF corrected triplet states showed there are four ISC pathway below 30000 cm^{-1}, which also are solvent dependent. The solvent dependence of the energy gap between the singlet and triplet excited states, ΔE(T-S; ε) = E(triplet; ε)-E(singlet; ε), decreases with increase of solvent dielectric constant up to acetone and remain almost constant with further increase of ε. For instance, when molecular environment changes from gas-phase to acetone medium, the computed energy gap (ΔE(T-S; ε)) between the closest singlet and triplet state changes from −2602 to −2458 cm^{-1} (T_2-Q), from 3269 to 2138 cm^{-1} (T_3-Q), from 743 to 208 cm^{-1} (T_5-B), from 348 to 65 cm^{-1} (T_{11}-L1), from 373 to 105 cm^{-1} (T_{12}-L2), from 1076 to 5 cm^{-1} (T_{17}-M) and from 1375 to 151 cm^{-1} (T_{18}-M).

3.3 Solvent dependence of TSPP

Akins *et al.* [60] and Zhang *et al*. [61] also have measured the UV–vis spectra of the free-base TSPP and the H_4TSPP (diprotonated- or dianionic-TSPP). The author reported that the absorption spectrum of the TSPP exhibited Q(0-0)-bands at about 517 (± 2) and 640 (± 3) nm and the B-band at ~412 nm, the H_4TSPP spectrum revealed a weak broad Q(0-0)-band at 645 nm and an intense B-band at 432 nm. Furthermore, the UV–vis spectra of the singlet TSPP and H_4TSPP in the region of 420-460 nm indicated that the maximum peak position of the B-band in the ethanol, methanol, and DMSO solvents is red shifted with respect to water [62].

The excited-state dynamics of the TSPP has been experimentally studied by several research groups. The lowest triplet state (T_1) of the TSPP has been observed at 862 nm [63] and the energy gap between the Q1 band and the T_1 state in the TSPP, ΔE(T_1-Q1), is measured to be about 4000 cm^{-1} (48 kJ mol^{-1}) [64]. Moreover, the measured triplet–triplet absorption spectrum of the TSPP (at pH = 7) exhibited a strong peak between 440 and 450 nm with a three weak transitions: at 524 ± 2 nm, a broad peak between

ca. 550-575 nm and third one at 624 nm [65]. For the H_4TSPP (at pH = 3), their triplet-triplet absorption spectrum in the range of 450-700 nm displayed two relatively strong and one weak peaks. Their estimated peak positions: at ~500 ± 2 nm with a shoulder (at about 530 nm) and 650 ± 5 nm; a weak one at about 596 ± 2 nm. Jirsa and *et al*. also observed a strong triplet band at 444 nm in the TSPP absorption spectrum [66].

Our calculated dipole allowed singlet-singlet and triplet-triplet electronic transition energies of the TSPP and H_4TSPP are in good agreement with these experimentally observed absorption spectra discussed above. The results from calculations show that the spectral position of the calculated absorption bands gradually change as a function of solvent dielectric constant only in the region of ε = 1 to about 20.493 (acetone) and remain unchanged with further increase of ε. Thus, we only discuss the shifts in the band position when molecular environment changes from gas phase to acetone medium and the results may be summarized as follows.

Singlet TSPP: The solvent-dependence of dipole allowed singlet-singlet electronic transition energies of TSPP is given in **Figure 5A**. **Figure 5B** shows the shifts in band positions caused by solvent, which is similar to the shifts in the TPP absorption spectra. As seen in **Figure 5A** and **B**, the bands at 17064 cm^{-1} (Q1, 586.0 nm) and 18178 cm^{-1} (Q2, 550.1 nm) in the gas phase spectrum of singlet TSPP are 576 and 541 cm^{-1} blue-shifted to 17365 cm^{-1} (575.9 nm) and 18467 cm^{-1} (541.5 nm), respectively; however, the Soret-bands B1 at 24692 cm^{-1} (405.0 nm) and B2 at 25060 cm^{-1} (399.0 nm) in gas phase spectrum are substantially shifted as function of increasing ε up to about 20.493, such as are first 958 and 1112 cm^{-1} red shifted to 23734 cm^{-1} (421.3 nm) and 23948 cm^{-1} (417.6 nm) with increase of solvent dielectric constant ε from 1.0 to 5.32, and which are then turned to increase up to 24429 cm^{-1} (409.3 nm) and 24758 cm^{-1} (403.9 nm) with increase of ε from 5.32 to about 20.493. With further increasing value of ε, they remain constant within ±120 cm^{-1} fluctuation. The bands at 26319 cm^{-1} (labeled as L1 at 380.0 nm) in the gas phase spectrum is shifted to 28117 cm^{-1} (355.7 nm) in the same region.

Triplet TSPP: The solvent-dependence of the triplet-triplet vertical electronic transition energies of the TSPP is similar to these in the triplet-TPP spectrum when molecular environment changes from gas phase to solvent phase. For instance, the SCF-corrected the lowest triplet state at 10922 cm^{-1} (915.6 nm) exhibits a exponentially blue shift up to around 11426 cm^{-1} (875.2 nm) as function of the ε (up to 20.493), which then

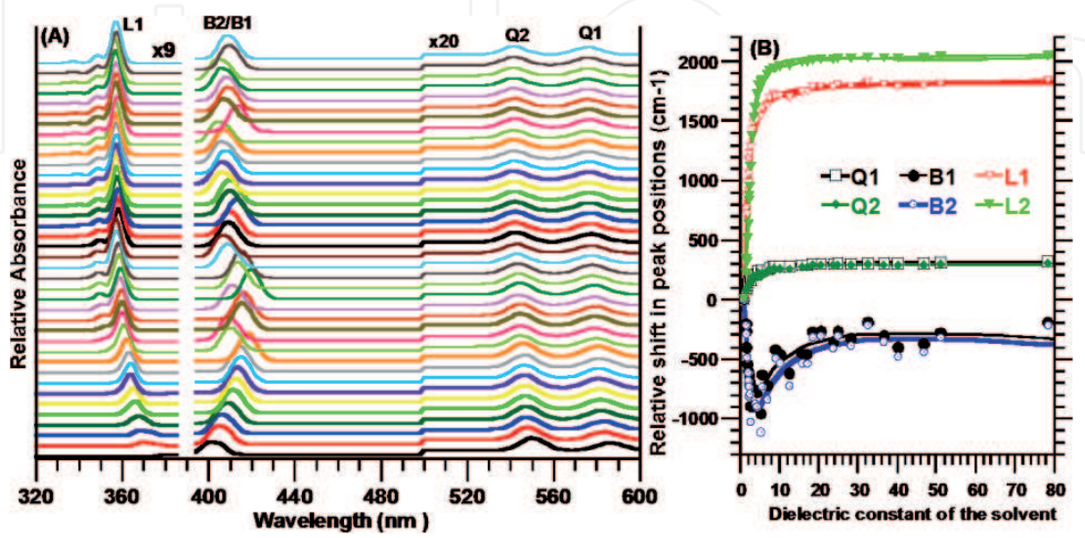

Figure 5.
(A) The calculated solvent-dependence of the singlet-singlet electronic absorption spectrum of the TSPP in the thirty-nine different environments, where the dielectric constant of the molecular environment increases from bottom (ε = 1.00) to top (ε = 181.560); (B): The red-shifts in the absorption band positions as function of dielectric constant of the solvent (ε), reference to their corresponding values in gas-phase spectrum.

remains almost constant within 20 cm^{-1} with the further increase in ε. This predicted value of the T_1 (lowest triplet state) in the solvent with its dielectric constant value $\varepsilon \geq 20.493$ is consistent with its experimental value of 862 nm as mentioned above.

As seen in **Figure 6A** and **B**, the calculated dependence of the dipole triplet-triplet vertical dipole allowed electronic transitions ($T_1 \rightarrow T_n$) energies also exhibits a exponentially red/blue-shifts as function of the ε. The triplet absorption spectrum displays the maximum shifts in acetone as solvent. For example, while the T_7 at 14980 cm^{-1} (667.5 nm), T_8 at 15282 cm^{-1} (654.4 nm) and T_{17} at 18757 cm^{-1} (533.1 nm) in the gas phase spectrum of the TSPP are respectively 2415, 2177 and 902 cm^{-1} blue-shifted (to 17295 cm^{-1} (574.9 nm), 17459 cm^{-1} (572.8 nm) and 19659 cm^{-1} (508.7 nm)) in acetone medium, the T_{24} at 22000 cm^{-1} (454.5 nm) in gas phase is 1036 cm^{-1} red-shifted to 20964 cm^{-1} (477.0 nm).

In the same region, T_4, T_5, T_9 and T_{12} states displayed a relatively weak solvent dependence such as while the triplet states T_4 (13248 cm^{-1}/754.8 nm) and T_{12} (18236 cm^{-1}/548.4 nm) display a maximum blue-shift of about 500 cm^{-1}; the T_5 (14022 cm^{-1}/713.2 nm) and T_9 (18230 cm^{-1}/548.6 nm) triplet states exhibit about 400 cm^{-1} red-shift (**Figure 6B**).

For a possible inter system crossing (ISC) process, we also examined the solvent effect on the energy-gap between the closest singlet and the triplet states, ΔE(S-T, ISC) = E(T) - E(S). The singlet states Q2, B2 and L2 singlet states are almost overlapping with the T_3 (triplet-triplet forbidden state), T_4 and T_8 triplet states, respectively. For instance, with changes solve ε = 1 to 20.493, ΔE(S-T, ISC) the energy-gap changes from: 234 to −40 cm^{-1} between the Q2 and T_3 state; −2108 to −1829 cm^{-1} (Q1 and T_2); −3322 to −2931 cm^{-1} (Q2 and T_2); 234 to −40 cm^{-1} (Q2 and T_3); −522 to 510 cm^{-1} (B1 and T_4); −890 to 181 cm^{-1} (B2 and T_4); −115 to 767 cm^{-1} (L1 and T_8); and − 576 to 87 cm^{-1} (L2 and T_8) with going from ε = 1 to 20.493. With the further increase in ε, they remain nearly unchanged within a few ten wavenumber variations.

3.4 Solvent dependence of the H_4TSPP

Singlet H_4TSPP: The results from calculations shows that the solvent effect on the dipole allowed vertical electronic transition energies of the H_4TSPP is similar to

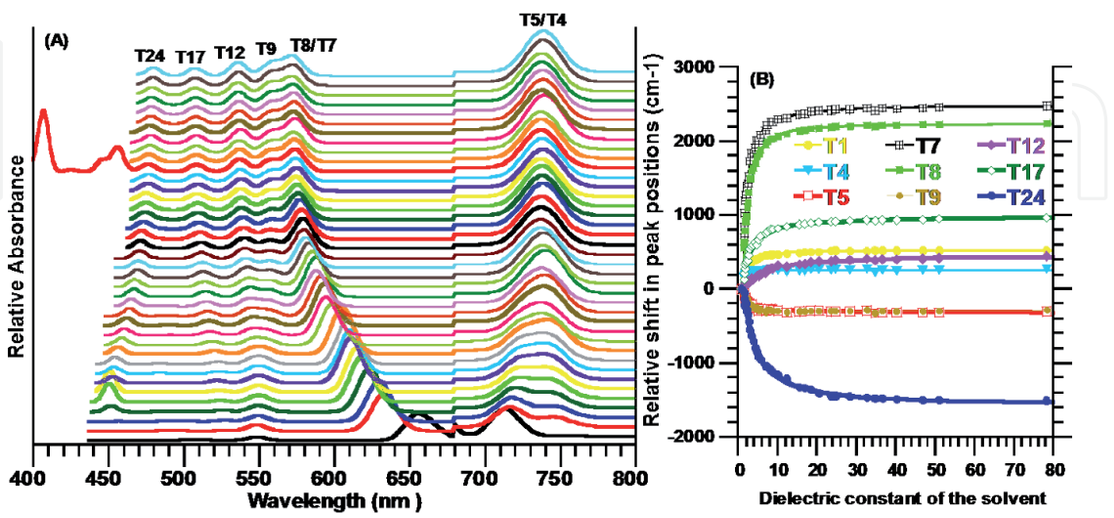

Figure 6.
(A) The calculated solvent-dependence of the triplet-triplet electronic absorption spectrum of the TSPP in the thirty-nine different environments, where the dielectric constant of the molecular environment increases from bottom (ε = 1.00) to top (ε = 181.560); (B): The shift in the energy level of the T_n state reference to their corresponding value in gas-phase spectrum as function of dielectric constant of the solvent (ε). The shift in the energy level of the T_1 state is obtained using the equation: $\Delta E(T_1,\varepsilon) = E(T_1,\varepsilon)-E(S_0,\varepsilon)$.

these in the singlet-TSPP spectrum, but exhibit more stronger blue-shift. As seen in **Figure 7A** and **B**, with increasing value of ε from 1.00 to about 20.493, the nearly degenerated Q-bands predicted at 10692/10737 cm^{-1} (935.3/932.4 nm) in gas-phase exhibit extremely blue-shift with the increase of ε such as are respectively blue-shift to 15173/15188 cm^{-1} (659.1/658.4 nm) in acetone as solvent with ε = 20.493 and to 155304/15317 cm^{-1} (or 653.4/652.9 nm) in water (ε = 78.355).

Likewise, the nearly degenerated B-bands at 12720/12796 cm^{-1} (or 786.1/781.5 nm) in gas phase spectrum are respectively 9839/9755 cm^{-1} blue shifted to 22559/22551 cm^{-1} (443.3/443.4 nm) in acetone (ε =20.493) and to 22755/22751 cm^{-1} (439.5/439.5 nm) in water (ε =78.355). Relatively very weak bands with relatively weak intensity (labeled as L-bans) at 14211/14189 cm^{-1} (703.7/704.8 nm) are substantially blue-shifted (9139/9108 cm^{-1}) to 23350/23297 cm^{-1} (428.3/429.2 nm) in acetone and to 23907/23861 cm^{-1} (528.2/528.2 nm) in water, respectively.

In literature, we could not find an experimentally observed electronic spectrum of H_4TSPP in the gas-phase or in a less polar solvent environment to compare with our calculated results. In high polar or acidic solutions, the observed B- and Q-bands in the electronic spectra of H_4TSPP have been published by several researchers as discussed in the TSPP section, which are in agreement with the results presented here. Furthermore, results also shows that the stability of the electronic spectrum of the diprotonated TSPP (H_4TSPP) rapidly increases with increasing polarity or dielectric constant of the solvent (**Figure 7A** and **B**).

Triplet H_4TSPP: The calculations predicted the lowest triplet state (T_1) at 5046 cm^{-1} (1982 nm) in gas phase shifts toward shorter wavelength region with increasing value of ε from 1 to 28.29, and stay almost unchanged around 880 cm^{-1} (1136 nm) with the further increase in ε. The calculated triplet-triplet electronic transition energies of the H_4TSPP exhibit strong solvent-dependence in the range of solvent dielectric constant ε from 1.00 to 28.29. As seen in **Figure 8A** and **B**, the dipole allowed vertical electronic transition energies from the T_1 state to T_4, T_9, T_{11} and T_{12} triplet states are substantially blue shifted to 12047, 13554, 14359, and 15959 cm^{-1} (or 830.1, 737.8, 696.5 and 626.6 nm) from 6332, 8707, 12784 and 11947 cm^{-1} (or 1579, 1149, 782 and 837 nm) in the gas phase, respectively.

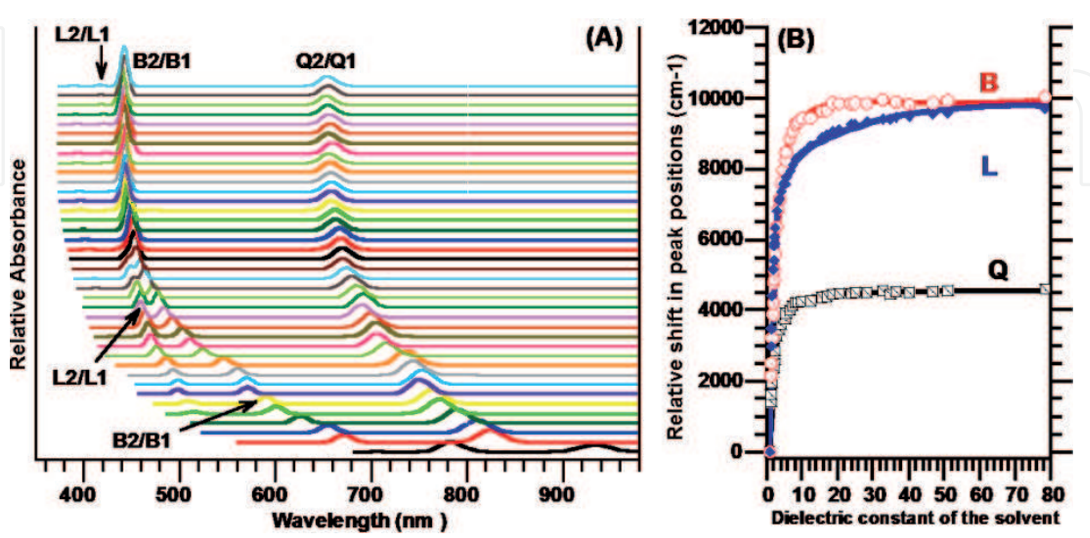

Figure 7.
(A) The calculated solvent-dependence of the singlet-singlet electronic absorption spectrum of the H_4TSPP in the thirty-nine different environments, where the dielectric constant of the molecular environment increases from bottom (ε = 1.00) to top (ε = 181.560); (B): The red-shifts in the absorption band positions as function of dielectric constant of the solvent (ε), reference to their corresponding values in gas-phase spectrum.

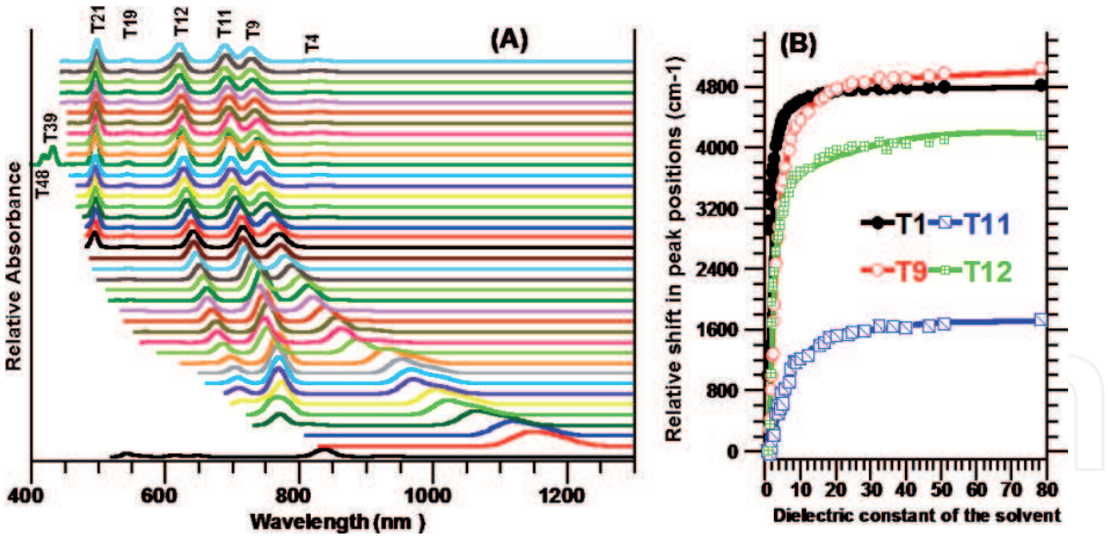

Figure 8.
(A) The calculated solvent-dependence of the triplet-triplet electronic absorption spectrum of the H_4TSPP in the thirty-nine different environments, where the dielectric constant of the molecular environment increases from bottom (ε = 1.00) to top (ε = 181.560); (B): The shift in the energy level of the T_n state reference to their corresponding value in gas-phase spectrum as function of dielectric constant of the solvent (ε). The shift in the energy level of the T_1 state is obtained using the equation: $\Delta E(T_1,\varepsilon) = E(T_1,\varepsilon)-E(S_0,\varepsilon)$.

The solvent-dependency of the smallest energy gap between the singlet and SCF corrected-triplet states, ΔE(singlet-triplet, ε), are estimated to be around 2300 cm^{-1} (T4-Q states) and about 300 ± 150 cm^{-1} (T9-B) and (T11-L).

4. Conclusion

Results from calculated electronic spectra of the TPP, TSPP and their diprotonated structures in gas-phase and thirty eight different solvent showed that solvent gives rise to a blue/red shifts in the singlet-singlet and triplet-triplet dipole allowed vertical electronic transition energies as a function of solvent dielectric constant only in the region of ε = 1 to about 20.493 (acetone), but no significant spectral shifts found for the solvent dielectric constant ε ≥ about 20.493.

In the low energy region (Q-band region), the Q-bands of the TPP first exhibit a red-shift (of about 70 cm^{-1}) with increasing solvent dielectric constant up to ε = 5.32 (diiodomethane) and then to a blue shift with increasing of the ε (from 5.32 to 20.493), However, the Q-bands of the TSPP display only a blue shift (as much as 295 cm^{-1}) with increasing of solvent dielectric constant up to 20.493. The Q-bands in both H_4TPP and H_4TSPP spectra exhibits a rapid blue-shift with increasing of solvent dielectric constant, but the shifts in the H_4TSPP is much stronger than that in the H_4TPP spectrum; such as 4480 cm^{-1} in the H_4TSPP and 490 cm^{-1} in the H_4TPP in acetone as solvent.

In the high energy region, the solvent effect on the Soret band (B-band) of the TPP is stronger than on that of the TSPP. The B-band of both molecules first display a red-shift in range from 1 to 5.32 and then turn to blue shift up to acetone (ε = 20.493). In both H_4TPP and H_4TSPP compounds, the B-band exhibit a strong blue-shift with increase of ε, but the shift in the B-band position of H_4TSPP is much stronger than that of the H_4TPP. With the further increase of the solvent dielectric constant (ε), spectral position of the Q- and B-bands become almost stabile within a few-tens wavenumber ranges. Furthermore, the intensity of the B-band slightly increases with increase of solvent dielectric constant.

The solvent results in both red- and blue-shifts in the triplet-triplet transition energies in the TPP, H_4TPP and TSPP spectra in the calculated spectral region, but only blue-shift takes place in the H_4TSPP. Furthermore, the calculations also showed that the ISC process many not only take place between the Q-bands and the nearest triplet states, but also it is possible between the B- and L-bands and the nearest triplet states because these singlet states almost overlapping with the higher triplet states. Therefore, the ISC may occurs in the singlet state B (or B-band) via surface touching, based on the competition between the IC (from the B- to Q-bands) and the ISC process. This energy gaps between Q/B-bands and the nearest triplet states is also solvent dependent for $\varepsilon < 20$.

The results of calculations also indicate that solvent effect on the nonplanar macrocycle conformation of porphyrin (H_4TPP/H_4TSPP) is more significant than that on the planar macrocycle conformation of porphyrin (TPP/TSPP). This observation suggest that the nonplanar macrocycle conformation increase the electrostatic/electronic interaction between the four hydrogen atoms at the macrocycle core and molecular environment.

The results from calculations suggest that the polarized porphyrin molecule may interact strongly with increasing solvent polarity and lead to modification of dipole allowed vertical electronic transition energies with increasing solvent polarity arising from partial charge transfer between solvent and the porphyrin macrocycle and/or the intramolecular charge transfer. Moreover, in terms of the electronic configuration of the molecular orbitals of the porphyrin, the additional charge partially may occupy a nonbonding and/or antibonding orbitals that brings about the weakening of the chemical bonding in porphyrin. Also, the partial charge transfer from an occupied nonbonding (atomic orbital of the N atom) and/or antibonding orbital results in the strengthening of the chemical bonding in porphyrin. The change in occupancy of the bonding/nonbonding orbitals affect the electronic excited state, which gives rise to shift in the electronic absorption spectrum of the porphyrin molecule.

As a result, the solvent-dependence of the spectroscopic features of porphyrin can be used to monitor micro environmental changes of porphyrin-like compounds incorporated in biological systems and nanoparticles, which also may be appropriate for study and monitoring changes of the chemical environment in different solutions and interactions in biological systems, as well as deal with nonspecific *adsorption on nanomaterials* and their orientations on the surface, which is very important for the *Surface-Enhanced Resonance Raman Scattering* (SERRS) and Aggregation-Enhanced Raman Scattering (AERS) in different solvent. Furthermore, such strongly solvent-dependent electronic bands can be used as a marker of the environmental dielectric constant.

Acknowledgements

We would like to thank TUBITAK ULAKBIM, High Performance and GridComputing Center (TR-Grid e-Infrastructure) for the calculations reported in the theoretical part of this paper.

Author details

Metin Aydin
Department of Chemistry, Faculty of Art and Sciences, Ondokuz Mayis University, Samsun, Turkey

*Address all correspondence to: aydn123@netscape.net

References

[1] Dolphin, D. (Ed.) The Porphyrins; *Academic Press*: New York; Vol. 1-3, **1978/1979**

[2] M. Gouterman (Ed.). Porphyrins: Excited States and Dynamics. ACS Symp. 321, *American Chem. Soc*.: Washington D. C., **1986**.

[3] Ojima, I. (Ed.) Catalytic Asymmetric Synthesis; Vett Publisher Inc.: New York, **1993**.

[4] Kadish, K. M.; Smith, K. M.; Guilard (Eds.) R. The Porphyrin Handbook; *Academic Press*: New York, Vols. 1-10, **2000**.

[5] Kadish, K. M.; Smith, K. M.; Guilard, R. Handbook of Porphyrin. *Science* **2011**, 14, 249

[6] Holten, D.; Bocian, D. F.; Lindsey, J. S. Probing Electronic Communication in Covalently Linked Multiporphyrin Arrays. A Guide to the Rational Design of Molecular Photonic Devices. *Acc. Chem. Res.*, **2002**, 35 (1), 57-69

[7] Hopfield, J.J., Onuchic, J.N. & Beratan, D.N. A molecular shift register based on electron transfer. Science **1988**, 241, 817-820.

[8] Bonnett, R. Photosensitizers of the porphyrin and phthalocyanine series for photodynamic theory. Chem. Soc. Rev. **1995**, 24, 19-33.

[9] Andrade, S. M.; Costa, S. M. B. Spectroscopic Studies on the Interaction of a Water Soluble Porphyrin and Two Drug Carrier Proteins. Biophysical Journal **2002**, 82, 1607-1619.

[10] Ben-Hur, E.; Horowitz, B. Advances in photochemical approaches for blood sterilization. Photochem. Photobiol. **1995**, 62, 383-388.

[11] Uhehara, K.; Hioki, Y,; Mimuro. M. The chlorophyll *a* aggregate absorbing near 685 nm is selectively formed in aqueous tetrahydrofuran. *Photochem. Photobiol.* **1993**, 58, 127-132.

[12] Tominaga, T. T.; Yushmanov, V. E; Borissevitch, I. E.; Imasato, H; Tabak. M. Aggregation phenomena in the complexes of iron tetraphenylporphine sulfonate with bovine serum albumin. *J. Inorg. Biochem*. **1997**.

[13] Togashi, D. M., and S. M. B. Costa. Absorption, fluorescence and transient triplet-triplet absorption spectra of zinc tetramethylpyridylporphyrin in reverse micelles and microemulsions of aerosol OT–(AOT). Phys. Chem. Chem. Phys. **2000**, 2, 5437-5444.

[14] Dolphin (Ed.), D. The Porphyrins; *Academic Press*, New York; Vol. 1-3, **1978/1979**.

[15] Ferreira, G. C (Ed.); Kadish, K. M.; Smith, K. M.; Guilard, R. Handbook of Porphyrin Science (Volumes 26 – 30) *World Scientific Publishing Company*, **2013**.

[16] Tsvirko, M.P.: Solovjev, K.N.; Gradyushko, A.T.; Dvornikov, S.S. Phosphorescence of porphyrin free bases and their complexes with light metals. *Opt. Spectrosc*. **1975**, 38, 400-404.

[17] Volker, S.; van der Waals, J.H. Laser-induced photochemical isomerization of free base porphyrin in an *n*-octane crystal at 4·2 K. Mol. Phys. **1976**, 32, 1703-1718.

[18] Loboda, O. Quantum-chemical studies on Porphyrins, Fullerenes and Carbon Nanostructures; Springer Science & Business Media, **2012**.

[19] Aydin, M. (2014). Comparative study of the structural and vibroelectronic properties of porphyrin and its derivatives. Molecules. **2014**, *19*, 20988-21021.

[20] Gouterman, M. Spectra of porphyrins. J. Mol. Spectrosc. **1961**, 6, 138-163.

[21] Parusel, A.B.J.; Grimme, S. DFT/MRCI calculations on the excited states of porphyrin, hydroporphyrins, etrazaporphyrins and metalloporphyrins J. Porphyrins Phtalocyanines, **2001 5**, 225-232.

[22] Nakatsuji, H.; Hasegawa, J.; Hada, M. Excited and ionized states of free base porphin studied by the symmetry adapted cluster-configuration interaction (SAC-CI) method. J. Chem. Phys. **1996**, 104, 2321.

[23] Hasegawa, J.; Ozeki, Y.; Hada, M.; Nakatsuji, H. Theoretical Study of the Excited States of Chlorin, Bacteriochlorin, Pheophytin *a*, and Chlorophyll *a* by the SAC/SAC−CI Method. *J. Phys. Chem*. B. **1998**, 102, 1320-1326.

[24] Serrano-Andres, L.; Merchan, M.; Rubio, M.; Roos, B.O. Interpretation of the electronic absorption spectrum of free base porphin by using multiconfigurational second-order perturbation theory. Chem. Phys. Lett. 1998, 295, 195-205

[25] Sundholm, D. Density functional theory calculations of the visible spectrum of chlorophyll *a*. Chem. Phys. Lett. 1999, 302, 480-484.

[26] Sundholm, D. Interpretation of the electronic absorption spectrum of free-base porphin using time-dependent density-functional theory. Phys. Chem. Chem. Phys. **2000**, 2, 2275-2281.

[27] Sundholm, D. Density functional theory study of the electronic absorption spectrum of Mg-porphyrin and Mg-etioporphyrin-I. Chem. Phys. Lett. **2000**, 317, 392-399.

[28] Nguyen, K.A.; Day, P.N.; Pachter, R. Triplet Excited States of Free-Base Porphin and Its β-Octahalogenated Derivatives. J. Phys. Chem. A. **2000**, 104, 4748-4754.

[29] Aydin, M. DFT and Raman spectroscopy of porphyrin derivatives: Tetraphenylporphine (TPP). Vib. Spectrosc. **2013**, 68, 141–152.

[30] Jun Takeda and Mitsuo Sato. Unusual solvent effect on absorption spectra of nonplanar dodecaphenylporphyrin caused by hydrogen-bonding interactions. Chemistry Letters 1995, 971-972.

[31] Li, Y. Solvent effects on photophysical properties of copper and zinc porphyrins. Chin. Sci. Bull. 53 (2008) 3615-3619.

[32] J. Tomasi, B. Mennucci, and R. Cammi. Quantum Mechanical Continuum Solvation Models. Chem. Rev. 105 (2005) 2999-3093.

[33] M. Milovanovic. Experimental and theoretical approaches coupled with thermochemistry of reactions in solution and role of non-covalent interactions. PhD. Thesis, Doctoral School of Chemical Science, University of Strasburg, Faculty of Chemistry, 2018, France.

[34] J. Tomasi and M. Persico. Molecular interactions in solution: An overview of methods based on continuous distributions of the solvent. Chem Rev. 94 (1994) 2027-2094.

[35] I. Izumi, Y. Atshi and K. Takayoshi. Solvent effect for ruthenium porphyrin. Sci China Phys Mech Astron. 53(6) (2010) 1005-1012.

[36] S. H. Saraf and R. Ghiasi. Effect of the Solvent Polarity on the Optical Properties in the (OC)5Cr=(OEt)(Ph) Complex: A Quantum Chemical Study. Russian Journal of Physical Chemistry A, 2020, Vol. 94, No. 5, pp. 1047-1052.

[37] S. Kamrava, R. Ghiasi and A. Marjani. Structure, electronic properties and slippage of cyclopentadienyl and indenyl ligands in the (η^5-C_5H_5) (η^3-C_5H_5) $W(CO)_2$ and (η^5-C_9H_7) (η^3-C_9H_7) $W(CO)_2$ complexes: A C-PCM investigation. Journal of Molecular Liquids 329 (2021) 115535.

[38] L. Edwards, D.H. Dolphin, M. Gouterman, A.D. Adler, Porphyrins XVII. Vapor absorption spectra and redox reactions: Tetraphenylporphins and porphin. J. Mol. Spectrosc. 38 (1971) 16-32.

[39] M. Aydin and D. L. Akins. DFT studies on solvent dependence of electronic absorption spectra of free-base and protonated porphyrin. Computational and Theoretical Chemistry 1132 (2018) 12-22.

[40] Metin Aydin and Daniel L. Akins (October 5th 2016). Geometric and Electronic Properties of Porphyrin and its Derivatives, Applications of Molecular Spectroscopy to Current Research in the Chemical and Biological Sciences, Mark T. Stauffer, IntechOpen, DOI: 10.5772/64583.

[41] Frisch, M. J.; Trucks, G. W.; Schlegel, H. B.; Scuseria, G. E.; *et al*. Gaussian 09 Revision A.02.

[42] Becke, A. D. Density-Functional Thermochemistry. III. The Role of Exact Exchange. J. Chem. Phys. **1993**, 98, 5648–5652.

[43] Lee, C.; Yang, W.; Parr, R. G. Development of the Colle-Salvetti Correlation-Energy Formula into a Functional of the Electron Density. Phys. Rev. B **1988**, 37, 785–789.

[44] Krishnan, R.; Binkley, J. S.; Seeger, R.; Pople, J. A. Self-consistent molecular orbital methods. XX. A basis set for correlated wave functions. *J. Chem. Phys.* **1980**, *72*, 650-654.

[45] Tomasi, J.; Mennucci, B.; Cammi, R. Quantum Mechanical Continuum Solvation Models. Chem. Rev. **2005**, 105, 2999–3093.

[46] Barone, V.; Cossi, M. Quantum Calculation of Molecular Energies and Energy Gradients in Solution by a Conductor Solvent Model. J. Phys. Chem. A **1998**, 102, 1995-2001.

[47] Miertus, S.; Scrocco, E.; Tomasi, J. Electrostatic Interaction of a Solute with a Continuum. A Direct Utilization of ab Initio Molecular Potentials for the Prevision of Solvent Effects. Chem. Phys. **1981**, 55, 117–129.

[48] Cossi, M.; Rega, N.; Scalmani, G.; Barone, V. Energies, structures, and electronic properties of molecules in solution with the C-PCM solvation model. J. Comput. Chem. **2003**, 24, 669–681.

[49] N. M. O'Boyle, J. G. Vos, GaussSum 0.8; Dublin City University: Dublin, Ireland, (**2004**). Available at http://gaussum.sourceforge.net.

[50] Even, U.; Magen, J.; Jortner, J.; Friedman, J. M.; Levanon, H. Isolated ultracold porphyrins in supersonic expansions. I. Free-base tetraphenylporphyrin and Zn-tetraphenylporphyrin. *J. Chem. Phys.* **1982**, *77*, 4374-4383.

[51] Benthem, L. Tetraphenylporphyrin dimers: An optical and magnetic resonance study. Thesis Wageningen Agricultural University, Neitherlands, **1984**.

[52] Badger, G.M.; Jones, R.A.; Laslett, R.L. Porphyrins. VII. The synthesis of porphyrins by the Rothemund reaction. *Aust. J.* Chem. 1964, 17, 1028-1035.

[53] Harriman, A. Luminescence of porphyrins and metalloporphyrins. Part 1.—Zinc(II), nickel(II) and manganese(II) porphyrins. *J. Chem.*

Soc., Faraday Trans. 1, **1980, 76,** 1978-1985.

[54] Egorova, G.D.; Knyukshto, V.N.; Solovev, K.N.; Tsvirko, M.P. Intramolecular spin-orbital perturbations in ortho- and meta-halogeno-derivatives of tetraphenylporphin. Opt. Spectrosc. (USSR). **1980**, 48, 602-607.

[55] Pekkarinen, L.; Linschitz, H. Studies on Metastable States of Porphyrins. II. Spectra and Decay Kinetics of Tetraphenylporphine, Zinc Tetraphenylporphine and Bacteriochlorophyll[1]. *J. Am.* Chem. Soc. 1**960**, 82, 2407-2411.

[56] Liu, Z. B.; Zhu, Y.; Zhu, Y. Z.; Tian, J. G.; Zheng, J. Y. Study on Nonlinear Spectroscopy of Tetraphenylporphyrin and Dithiaporphyrin Diacids. J. Phys. Chem. B **2007,** *111,* 14136-14142.

[57] Okada, S.; Segawa, H. Substituent-Control Exciton in J-Aggregates of Protonated Water-Insoluble Porphyrins. J. AM. CHEM. SOC**. 2003**, 125, 2792-2796.

[58] Hasobe, T.; Fukuzumi, S.; Kamat, P. V. Ordered Assembly of Protonated Porphyrin Driven by Single-Wall Carbon Nanotubes. J- and H-Aggregates to Nanorods. *J. AM. CHEM. SOC.* **2005**, 127, 11884-11885.

[59] Zhang, Y.; Li, M. X.; Lu, M. Y.; Yang, R. H.; Liu, F.; and Li, K. A. Anion Chelation-Induced Porphyrin Protonation and Its Application for Chloride Anion Sensing. J. Phys. Chem. A **2005,** *109,* 7442-7448.

[60] Akins, D.L.; Özçelik, S.; Zhu, H.-R.; Guo, C. Fluorescence Decay Kinetics and Structure of Aggregated Tetrakis (p-Sulfonatophenyl)Porphyrin. J. Phys. Chem. **1996**, 100, 14390-14396.

[61] Zhang, Y.-H.; Chen, D.-M.; He, T.; Liu, F.-C. Raman and infrared spectral study of meso-sulfonatophenyl substituted porphyrins (TPPSn, n_/1, 2A, 2O, 3, 4). Spectrochim. Acta Part A. **2003**, *59*, 87-101

[62] Farajtabar, A.; Jaberi, F.; Gharib, F. Preferential solvation and solvation shell composition of free base and protonated 5, 10, 15, 20-tetrakis (4-sulfonatophenyl)porphyrin in aqueous organic mixed solvents. Spectrochimica Acta Part A. **2011**, 83, 213– 220.

[63] Roman Dedic. Antonın Svoboda, Jakub Psencık, Jan Hala, Phosphorescence of singlet oxygen and meso-tetra (4-sulfonatophenyl)porphin: Time and spectral resolved study. J. Mol. Struct. **2003**, 651-653, 301-304.

[64] Scholz, M.; Dedic, R. Thomas Breitenbach and Jan Hala. Singlet oxygen-sensitized delayed fluorescence of common water-soluble photosensitizers. Photochem. Photobiol. Sci., **2013**, 12, 1873-1884.

[65] Correa, D.S.; Boni, L. D.; Parra, G.G.; Misoguti, L.; Mendonça, C.R.; Borissevitch, I.E.; Zílio, S.C.; Neto, N.M.B.; Gonçalves, P.J. Excited-state absorption of meso-tetrasulfonato phenyl porphyrin: Effects of pH and micelles. Optical Materials. 2015, 42 516-521.

[66] Engst, P.; Kubat, P.; Jirsa, M. The influence of D20 on the photophysical properties of meso-tetra(4-sulphonatophenyl) porphine, Photosan III and tetrasulphonated aluminium and zinc phthalocyanines. J. Photo&em. Photobiol. A: Chem. *1994,* 78, 215-219.